

Expected Planet and False Positive Detection Rates for the Transiting Exoplanet Survey Satellite

Timothy M. Brown

Las Cumbres Observatory Global Telescope, Goleta, CA 93117

`tbrown@lcozt.net`

and

David W. Latham

Harvard-Smithsonian Center for Astrophysics, 60 Garden Street, Cambridge, MA 02138

`dlatham@cfa.harvard.edu`

ABSTRACT

The proposed Transiting Exoplanet Survey Satellite (TESS) will survey the entire sky to locate the nearest and brightest transiting extrasolar planets with orbital periods up to about 36 days. Here we estimate the number and kind of astrophysical false positives that TESS will report, along with the number of extrasolar planets. These estimates are then used to size the ground-based follow-up observing efforts needed to confirm and characterize the planets. We estimate that the needed observing resources will be about 1400 telescope-nights of imaging with 0.5m to 1m-class telescopes, 300 telescope-nights with 1m to 2m-class telescopes for the classification of the host stars and for radial velocity measurements with roughly 1 km s^{-1} precision, and 380 telescope-nights with 2m to 4m-class telescopes for radial velocity studies with precision of a few m s^{-1} . Follow-up spectroscopy of the smallest planets discovered by TESS at the best possible velocity precision will be limited by the number of telescope nights available on 4m to 10-m class telescopes with instruments such as HARPS and HIRES, but the pay-off of such efforts will be the determination of masses for Super Earths with sufficient accuracy to distinguish rocky desert planets from water worlds.

Subject headings: extrasolar planets, astronomical techniques

1. History and Motivation

Photometric surveys to detect transits by extrasolar planets have recently become a productive means of locating these objects (e.g., Koch et al. 1998; Alonso et al. 2004; Bakos et al. 2004; Baglin et al. 2007; Walker et al. 2003). All such surveys must deal with astrophysical false positives, i.e., periodic transit-like decreases in stellar brightness that arise from stars orbited by other stars, as opposed to stars orbited by planets. In most surveys these false positives outnumber those from planetary transits, often by factors of ten or more.

The proposed Transiting Exoplanet Survey Satellite (TESS) seeks to use an orbiting array of 6 small-aperture, wide-field CCD cameras (190 mm focal length $f/1.5$, with 18-degree square field of view) to survey the entire sky in a 2-year observing campaign, yielding a comprehensive list of transiting planets orbiting 2.5 million of the nearest stars. From a near-equatorial orbit, TESS will be able to observe the whole sky, and to detect objects with transit depths as small as 3×10^{-4} of the brightness of the parent star, with periods up to 36 days. These sensitivities will allow detection of Neptune-sized planets transiting Sun-like stars, and Super Earths around stars with radii some-

what smaller than the Sun’s. TESS was selected by NASA for Phase A in May 2008.

In order to size the ground-based follow-up effort needed to distinguish true planets from false positives, one must estimate the rates of false positives that TESS will produce. This paper describes how we made such estimates, and what we learned. The point of departure for our computations was the simulation code described by Brown (2003), which should be consulted for information about the computational strategy. Modifications to the code were needed to make estimates that were appropriate to TESS; the most important of these was the need to average the rates for line-of-sight triple star systems (two stars of which compose an eclipsing binary) over all Galactic latitudes. Lesser modifications brought the code up to date in terms of the period and radius distributions of presently-known extrasolar planets.

2. Categories of False Positives

Only a few physical processes cause most of the light variations that can masquerade as transits by planet-sized bodies. Each of these has its own characteristic distributions of transit depth, duration, and period, and each is (in principle) distinguishable from planetary transits by one or more kinds of follow-up observations. Examples of the methods typically used for ground-based transit surveys may be found in, e.g., O’Donovan et al. (2007) and Latham et al. (2008). The ones that are treated in this paper are described below.

Eclipsing binaries (EBs) in which the brighter object is a main-sequence star generate eclipses that have typical depths of tens of percent; these are usually so deep that confusion with transiting planets does not occur. But in a small fraction of cases, the eclipses are grazing, and eclipse depths can be a few percent or less. These grazing eclipses of stars can most easily be distinguished from those of planets if the light curve has high enough precision that the (generally flat-bottomed) eclipse shape generated by a planet can be distinguished from the (generally V-shaped) eclipses that result from stellar grazes. For transit observations with lower signal-to-noise ratio (S/N), the most powerful method for distinguishing EBs from planetary transits is to observe the radial velocity variations of the primary star. For

a stellar-mass companion, the orbital velocities are typically tens of km s^{-1} , while for planetary-mass companions, they are only hundreds of m s^{-1} at most. Thus high-resolution spectroscopy at modest S/N is an effective way to identify systems where stellar companions are responsible for the transit-like light curves. For example, radial velocities with a precision of 1 km s^{-1} are good enough to detect companions down to about 10 Jupiter masses for orbital periods of a few days around sun-like stars.

Eclipsing binaries in which the primary is a giant star usually have main-sequence companions, and it is not hard to find such pairs that yield eclipse depths similar to planetary transits. However, the eclipse duration for a dwarf eclipsing a giant tends to be much longer than for a planet transiting a dwarf, and this provides an effective way to distinguish between the two configurations. Furthermore, giants are typically too large to allow orbits with periods of just a few days, which is the domain favored by planets transiting sun-like stars. Spectroscopy of gravity-sensitive features such as the Mg b lines in the green is another effective way to identify host stars that are giants (Latham et al. 2008).

More difficult diagnostic problems arise if the light from an eclipsing binary is diluted by that from a brighter third star. An important class of these systems consists of an EB that, by chance, lies nearly along the same line of sight as an apparently brighter third star (we term these “line-of-sight triples”). When the third star dominates the light that we see, then moderate-sensitivity radial velocity measurements are likely to show no variability, consistent with the interpretation that the companion is a planet. The likelihood of random superpositions is larger than one might suppose, because transiting-planet surveys typically use very low spatial resolution, with stellar image diameters ranging from about 8 arcsec (for Kepler) to more than 30 arcsec (for most ground-based wide-angle surveys). To identify diluted systems of this sort, the easiest diagnostics involve improving the spatial resolution. One method that can be applied to the survey data itself is to use image subtraction to localize the variability associated with the system’s transits. If this center-of-variability does not coincide with the position of the nominal target star, then the variability is

likely to arise from a background eclipsing binary. Another powerful diagnostic method is to observe transits with much higher spatial resolution than that which was used to detect them. If the system is a line-of-sight triple, then the relatively large eclipses of the faint EB component will usually be easily observable if the EB is spatially resolved. Because the survey images are so large, seeing-limited resolution will often be enough to separate these systems. In extreme cases, however, adaptive optics (AO) observations or even high-resolution imaging from above the Earth’s atmosphere may be desirable.

Finally, and most difficult, one encounters gravitationally-bound triple systems (“physical triples”) that behave similarly to the line-of-sight triples just discussed. In the bulk of these cases, the angular separation between the EB system and the third star will be so small that they will remain spatially unresolved even with AO systems. In these cases, distinguishing planetary from stellar transits may be tackled using either photometry or spectroscopy. A photometric diagnostic is possible if the primary star of the EB system has a significantly different color than the third (brightest) star. If this is so, then the color of the triple system changes during eclipses – something that does not happen for planetary transits (O’Donovan et al. 2006). Lacking a sufficient color difference among the stars in the system, one must search for the small changes in spectral line shape that result from the weak line profiles from the EB system moving across the line profiles from the brightest star. Analysis of this sort can be difficult and time-consuming (Mandushev et al. 2005), especially if the lines of the EB have been broadened due to synchronization of the stellar rotation with a short orbital period by tidal mechanisms.

3. Adaptations for the TESS Calculation

The programs used here for estimating planet and false positive detection rates had previously been applied to small-aperture ground-based surveys and to NASA’s Kepler mission (Koch et al. 2004), in both cases with reference to restricted fields lying near the Galactic plane. Moreover, in the time since the previous calculations, knowledge of the distribution of exoplanet periods and radii has improved considerably. For calculations

specific to the circumstances of TESS, some modifications to the code were necessary.

The simplest adjustment was to set the confusion radius for line-of-sight triples to a value of 24 arcsec, appropriate to TESS’s 16-arcsec pixels and image performance. However, the probability that a bright foreground star will have a faint EB in its background depends not only on the detector’s confusion radius, but also on the areal density of stars. The latter is of course a strong function of Galactic latitude, and TESS’s all-sky nature thus requires allowance for this variation. For this reason we computed probabilities for line-of-sight triples for each 10-degree increment in the absolute value of the Galactic latitude, and then averaged the resulting probability distributions over latitude, weighting by the area of sky covered by each stripe.

Observations over the past few years have yielded a considerable amount of information about the distribution of planets with orbital period, and also (with substantial input from theory, eg. Ida & Lin (2005)) a schematic picture of the distribution with planetary radius. We therefore updated the parameterization used in Brown (2003). For the current purposes, we took the distributions in both planetary radius and orbital period to be such that equal cumulative probabilities are found in equal increments of the log of radius or period, respectively. We also took the joint probability distribution to be simply the product of the individual ones, i.e., we assumed that planetary radius and orbital period are independent variables. These distributions are broadly consistent with what we know about the real distributions of planetary parameters (e.g., Marcy et al. 2005; Udry & Santos 2007), but the latter are uncertain enough that we have not attempted a more sophisticated simulation. Indeed, one of the goals of TESS is to improve our knowledge of the rates of occurrence of planets as a function of planetary mass and length of semimajor axis.

4. Results

Given the assumptions outlined above, we computed the expected rates of planet detections and of the various kinds of false positives. For purposes of estimating total rates, we assumed that TESS would image 2.5×10^6 stars spanning Sloan r mag-

nitudes between 4.5 and 13.5, and we integrated over orbital periods between 1.0 and 36 days, transit depths between 10^{-4} and 0.04, and transit durations between 0.02 and 0.5 days. Counting only cases for which at least 3 transits could be observed, we arrived at the rates shown in Table 1. Note that this counting gave equal weight to transits of all depths down to the minimum of 10^{-4} . This signal level is appropriate for the brighter stars that TESS will observe, but is too optimistic by a factor of 3 or more for stars near the faint magnitude limit. As a result, Table 1 overestimates the numbers both of detected planets and of false positives. Because of the flat distribution of planets with the log of transit depth, this over-estimate for planets is probably about 20%. By similar reasoning, the over-estimate for line-of-sight triples is likely larger than for planets, and the over-estimates for EBs and physical triples are likely smaller.

4.1. Planets

The expected yield of planets is about 1700, or roughly one per 1500 stars surveyed. This number is considerably larger than that for ground-based surveys, a fact that we attribute mostly to TESS's superior photometric precision and consequent ability to detect smaller planets, but also to its regular and uninterrupted observing window function. The importance of photometric precision is illustrated in Figure 1, which shows the marginal probability distribution of planetary transit depths, and also of various false-positive sources. This distribution rises for decreasing transit depths starting at a relative depth of about 0.01, corresponding to transits of the largest likely planet (roughly Jupiter-sized) across the most common (roughly Sun-sized) star seen in small-aperture surveys. At shallower transit depths, the probability density per unit log depth becomes roughly constant. This behavior depends fairly sensitively on the assumed distributions of planetary radii and orbital semimajor axis, and the correlation between them. But given our assumptions about these distributions, it is clear that each increase of some factor in the minimum detectable transit depth yields about a constant increase in the number of detected planets.

The computed distribution of planetary periods rises monotonically from the longest to the

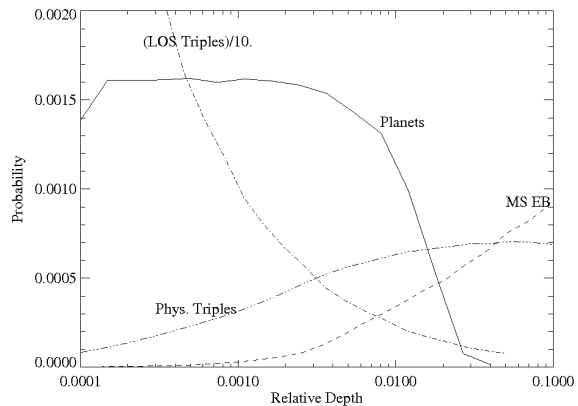


Fig. 1.— Probability density (per unit $\log \Delta$) for the occurrence of transits with relative depth Δ , for systems in which the transit is caused by a planet, by a grazing eclipse of a main-sequence star in an eclipsing binary, and by eclipses in EB systems that are diluted by light from a third star in a line-of-sight or a gravitationally-bound (physical) triple star system. The probability densities for line-of-sight triples have been divided by 10, to put them on a similar scale to the other curves. These are the marginal distributions, i.e., they have been integrated over all the other variables that describe each type of transit, namely orbital period, transit duration, and mass of the parent star.

TABLE 1
TRANSITING PLANET AND FALSE POSITIVE YIELDS

Signal Type	Number (3 Transits)
Planets	1687
MS Binaries	2111
Giant Binaries	40
Dilute MS Binaries	7237
Physical Triples	2080

shortest periods considered. As with ground-based searches, short-period planets are heavily favored for discovery, because of the relatively wide range of inclinations over which they exhibit transits. Between periods of 1 day and 30 days, the marginal probability density (per unit log period) falls by about a factor of 10.

The distribution of transit durations d is peaked at about 2 hours, and is nearly Gaussian when plotted against $\log d$, with a full width at half maximum of about 0.3 in $\log d$ (Figure 2). The typical transit is fairly short compared to the norm for known transiting planets because small, short-period planets are assumed to be both numerous and detectable.

4.2. Main Sequence Eclipsing Binaries

Ordinary eclipsing binaries in which both components are main-sequence stars will produce moderately numerous false positives, roughly equal in number to detected planets. The expected distribution of transit depth is, however, quite different from that of planets. The EB transit depth distribution peaks at about 25%, with a long tail to smaller depths caused by small stars transiting large ones, and by grazing transits (Figure 1). Moreover, the geometry of grazing transits implies that extreme grazes have short durations, and also that their light curves show distinctive V-shaped eclipses. Thus, with high-quality photometry, a large majority of these EB systems can be rejected as planets from an examination of their light curves. In addition, the EBs with short enough periods will show ellipsoidal variations in their light curves outside eclipses. The remaining cases will require follow-up medium-precision radial velocity measurements to distinguish them

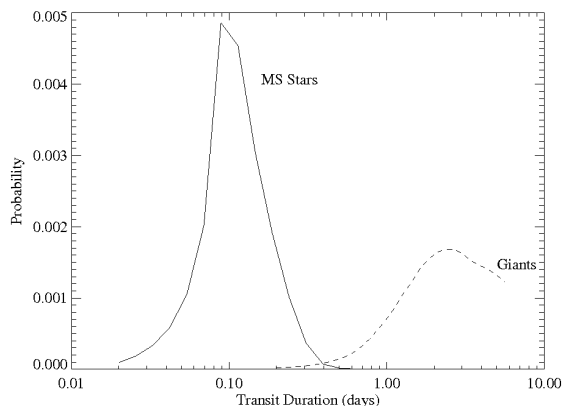


Fig. 2.— Probability density (per unit $\log d$) for the occurrence of a planet transiting a main-sequence star, or an eclipsing binary with a giant primary with a transit duration of d days. As before, these are marginal distributions, which in this case means that the joint probability distribution has been integrated over all values of eclipse depth, orbital period, and primary star mass (for planets) or $(B - V)$ color (for giants).

from planets.

4.3. Giant Eclipsing Binaries

Eclipsing binaries in which the brighter component is a giant will be a relatively unimportant source of false positives. This is mainly because the distribution of transit durations peaks at longer durations (about 2.5d) than is possible for planets in short-period orbits around roughly Sun-sized stars (Figure 2). Only a very small minority of grazing transits will produce light curve dips that are short enough to cause confusion with planets, and in these, a single spectrum of the object can reveal that the host star is a giant. These objects are therefore a negligible driver of the follow-up effort.

4.4. Line-of-Sight Triples

Line-of-sight triples will be the most numerous source of false positives encountered by TESS, being about 4 times more common than planetary transits. TESS’s large projected pixel size, and corresponding large radius of confusion, is the principal reason why this kind of false positive will be so important. In the simplest analysis (which is what we have done here), the distributions of orbital period and duration should be identical to those for main-sequence EBs, since line-of-sight triples consist of ordinary EB systems that happen to lie in nearly the same direction as a third, brighter star. According to this picture, the marginal probability density for transit depth rises monotonically as the depth decreases (Figure 1), because, in a homogeneous Galaxy, there are always many more faint EBs per square degree of sky than there are bright ones. This conclusion cannot be completely true, however, since the Galaxy is not homogeneous: at high Galactic latitudes, a very faint EB is almost certain to consist of a pair of red dwarfs, since more luminous stars would have to be far above the Galactic disk. Thus, in principle there should be differences from the naively-calculated probability densities for small apparent transit depth, due to the changing nature of the population of eclipsing stars. We acknowledge that such subtleties exist, but we have made no effort to model them here.

A powerful test for line-of-sight triples is to compare the position on the sky of the putative

planet-bearing star with that of the transit signal. This can be done first using data from the space-based transit search itself. The images from the TESS survey will have poor spatial resolution but high S/N; with difference-image analysis it will ordinarily be possible to localize the transit signal within a small fraction of a pixel.

The remainder will require detailed study of the shape and color of their light curves, as well as spectroscopy and high-resolution imaging, to identify the true source of the variations. Fortunately at this stage of the follow up, true planets should outnumber false positives by a considerable margin.

4.5. Physical Triples

Physical triple systems will be the most difficult of the false positive varieties to identify. They will be roughly as numerous as detected planets, and in at least some cases their observable characteristics will closely match those of plausible planetary systems. Figure 1 shows our estimated marginal probability distribution for transit depth Δ for these systems. The probability density (per unit $\log \Delta$) for this calculation peaks near transit depth $\Delta = 0.05$, but the distribution is very wide, with a tail that extends well below TESS’s sensitivity limit of 10^{-4} . One should recognize that the details of this distribution depend upon the poorly-known luminosity distributions within triple star systems; nevertheless both this model and observational experience (e.g., Mandushev et al. 2005) suggest that such triple systems can be a serious observational challenge.

Fortunately, a fairly large fraction of physical triples will have characteristics that do allow them to be distinguished from stars with transiting planets. Most EB configurations yield a V-shaped eclipse with such a long duration of ingress and egress that a transiting planet cannot be the cause. In many of the remaining cases, the brightest star in the system is a giant or a hot upper-main-sequence star, so that a single classification-quality spectrum can show that the eclipses must be highly diluted. In cases in which the third (brightest) star and the EB primary have sufficiently different temperatures, the transit depth becomes a function of wavelength – multicolor observations can then reveal the third star. If the flux ratio between the third star and the EB pri-

mary is not too large, a composite spectrum will be visible, and one set of lines will show Doppler shifts varying at the orbital period while the other set does not. Finally, if the flux ratio is large, and the stellar rotational speeds are such as to conceal the EB spectrum within that of the third star, one may nevertheless infer the third star’s presence from changes in spectral line asymmetries that are in phase with the eclipse period (Mandushev et al. 2005). Verifying this last behavior requires high-S/N spectroscopy at many orbital phases, and is therefore expensive in observing time.

5. Summary: Follow-up Requirements

As discussed above, several kinds of ground-based follow-up observations are feasible and useful, each with its own observing requirements and each able to identify different kinds of false positives. In this section we summarize the role of these false-positive tests in the context of TESS. To estimate the amount of follow-up observing time that will be needed, we must assign values for the fraction of impostors of different sorts that can be identified using each observing method. These estimates have various justifications, but sometimes the best we can offer are guesses, based in experience, but requiring considerable extrapolation. The reader should therefore treat the numerical estimates in the following paragraphs with caution.

The high-quality TESS photometry itself will allow us to identify some EBs and physical triples from the variability seen in their out-of-transit light curves. A crude guess based on our experience with ground-based surveys is that perhaps 20% of EBs and 10% of triples can be identified in this way. Comparing the centroid of the transit signal with that of the apparent host star, as described above, should be much more effective at sorting out line-of-sight triples, with a success rate that might reach 90%. This is because it should be possible to determine the relative position of the image centroid in and out of transit to a small fraction of the image size, roughly the FWHM divided by the S/N of the transit detection, assumed to be at least 7. Locating the positional offset during transit to a third of the image confusion radius should reduce the area allowed for an accidental alignment by an order of magnitude

Given a good ephemeris for a transiting candidate from the TESS photometry, searching for line-of-sight triples using seeing-limited ground-based imaging will also be very effective, and should require relatively little observing time per target. The eclipsing object in these apparent triples will usually be quite faint relative to the supposed planet host, but for this reason its eclipses must be relatively deep. A few observations inside and outside of the expected transit times thus should suffice to learn whether the varying star is the supposed planet host star or a faint neighbor. The large number of candidates for this type of follow-up observation should allow a multiplex strategy, where several objects can be followed up simultaneously. Assuming the images are seeing limited, we estimate that a further 90% of the line-of-sight triples remaining from the previous steps can be rejected by these observations, using about 0.5 hour total time on a 0.5-m class telescope for each target.

A single spectrum of gravity-sensitive features such as the Mg b lines in the green can immediately identify host stars that are giants. Luminous giants can be distinguished from dwarfs with surprisingly poor S/N, as low as 10 to 20 per spectral resolution element of 10 km s^{-1} (Latham et al. 2008). Subgiants, for example near spectral type G, are more difficult to distinguish from dwarfs, because their separation in radius/gravity/luminosity is smaller. The identification of short-period double-lined eclipsing binaries is often revealed by one or two high-resolution spectra with modest S/N, thus demonstrating that the transit-like light curves must be due to grazing eclipses in a system where the secondary is not too much fainter than the primary. Stars that are rotating much too rapidly to allow very precise radial velocity measurements can also be revealed by a single high-resolution spectrum at modest S/N.

We estimate the typical integration time for such spectra to be 10 to 20 minutes with 1m to 2m-class telescopes and modern spectrometers, and that this will allow discrimination of the roughly 15% of main-sequence EBs that show composite spectra, and most of the EBs and triple systems (both line-of-sight and physical) where the brightest star is a giant. Based on the relative numbers of giants and dwarfs among stars in TESS’s mag-

nitude range, we expect that about one-third of triple systems will be distinguishable in this way.

A few moderate-precision (i.e., 0.5 to 1 km s⁻¹) radial velocity measurements provide almost total rejection of the remaining undiluted eclipsing binaries. We assume that each target will require 2-4 radial velocity measurements, and that each of these spectra will also require 10 to 20 minutes of time on a 1m to 2m-class telescope. Experience suggests that these data will allow correct identification of 95% of EBs, 75% of Giant EBs, and two-thirds of triples (both line-of-sight and physical).

Accurate multicolor ground-based light curves provide a means of identifying a substantial fraction of the remaining diluted EB systems, namely the ones with deeper transits and big enough color differences between the EB and diluting star (such light curves are also necessary for characterizing the properties of genuine planets). These observations are relatively expensive in observing time because continuous coverage of full events is needed to achieve the necessary photometric precision, and one requires time resolution good enough to map out the shape of ingress and egress. Transit durations are typically 3 hours; to obtain satisfactory out-of-transit baselines, a typical transit event requires about 5 hours of telescope time. For relatively deep transit events (corresponding to giant planets), the precision achievable for single transit events with 0.5m to 1m-class telescopes will be adequate. Because of the demand for substantial telescope time, precise ground-based photometry is usually reserved for targets that have already been vetted by less demanding methods.

Ground-based photometry of single transit events has rarely achieved a photometric precision better than 1 mmag in sample times on the order of a few minutes. In a few cases larger ground-based telescopes have been used to push below 1 mmag (e.g., Johnson et al. 2008), and even better limiting precision has been demonstrated using a 1m-class telescope to observe multiple events (Winn et al. 2007). TESS will detect transits that are an order of magnitude shallower than can routinely be achieved from the ground. These will need to be followed up with space-based resources such as HST and JWST.

In a final step, remaining impostors may be revealed (and true planets characterized) by pre-

cise, multi-epoch, high-resolution Doppler spectroscopy. The high spectral resolution and S/N required for these measurements demands large telescopes, specialized highly stable spectrometers, and, for faint targets, long exposure times. To get 4 suitable spectra at the level of a few m s⁻¹ on these objects will require on the order 2 hours on 2m to 4m-class telescopes, and in some cases (such as stars with significant rotation or weak lines due to low metallicity or high temperature) significantly more. These observations are expensive and therefore are typically the last to be done, after all other means of rejecting false positives have been exhausted.

Last, it is worth noting that a few false positives are likely to slip through even the exhaustive vetting process just described, and be counted as planets. These are most likely to be special kinds of physical triple systems, in which the EB components are very faint relative to the brightest star. These will yield low-amplitude transits with light curves that are difficult to characterize from the ground. With a large brightness ratio between the brightest star and the EB primary, the orbital displacement of the EB spectrum lines will likewise be difficult to discern. At the same time, however, the blended line profiles may yield a Doppler signal that is plausible for a planet orbiting the brightest star. In short, given the vast number of double and multiple stars in the sky, one must expect that some of them will succeed in simulating planet-bearing single stars. It is difficult to estimate how often this will occur, but given the special circumstances required, we guess the number will be perhaps 20, or about 1% of the total sample of planets.

Table 2 shows the expected observing effort implied for the TESS experiment by the above hierarchy of follow-up observations. Rows in the table correspond to the various observational tests that can be performed. We assume that these are done in succession, with viable planet candidates passing to the next test, and likely false positives being removed from further consideration. The first 5 columns show the number of candidate transiting-planet systems that remain, going into each stage of the process, separated into true planets and the 4 different kinds of false positive. Column 6 shows the number of systems that must be observed at each stage, and column 7 shows the corresponding

number of observing hours (and the size of telescope facilities required).

The observations that reveal the largest numbers of false positives are detailed examination of TESS light curves and moderate precision radial velocity measurements. In both of these stages the total number of false positives is reduced by more than a factor of 2. Intermediate steps are also important, however. For instance, if spectroscopy is attempted before most of the line-of-sight triples have been weeded out, then one is likely to spend much observing time acquiring spectra of the wrong stars in these systems. The bulk of the observing time goes to the last 2 stages of the process, namely obtaining high-quality light curves and very precise radial velocity measurements. By the time the last stage is reached, our experience with ground-based surveys is that somewhat less than half of the candidates prove to be planets. The fraction of true planets should be larger than this for the TESS candidates, because in the relevant range of transit depth, the frequency of both main-sequence EBs and physical triples is a strongly decreasing function of depth, whereas that of planets is almost constant (see Fig. 1).

It is possible to realize some savings in the needed follow-up time by using existing multicolor photometry or astrometry (e.g. 2MASS or Tycho, Skrutskie et al. (2006); Høg et al. (2000)) to identify and discard giants from the TESS target list. Systems in which the light is dominated by a giant are almost always false positives, and there is no need to spend extra observing time determining to which category of false positive they belong.

The total observing time that can be saved by a pre-selection that eliminates giants is fairly modest, however. The largest contribution of such false positives comes from eclipsing binaries diluted by giants. Such systems should have a rate of occurrence similar to the fraction of giants in the field. For the magnitude limit of TESS, this fraction is about one-third.

In any case, most of the systems containing giants are eliminated early in the sifting process, at or before the step that calls for one classification-quality spectrum. These stages are relatively cheap in observing time. It is the true planets that must be followed all the way to the end of the decision tree, incurring high observing time costs

along the way. Finally, photometry or astrometry suitable for identifying giants is unavailable for most of the fainter stars in the TESS sample, and these are of course by far more numerous than the brighter ones. For example, only about 50,000 dwarfs out of TESS's sample of 2.5 million stars have Hipparcos parallaxes. Essentially all of the TESS targets will have 2MASS magnitudes, but with only 2MASS data, the giant-dwarf distinction is clear only for M stars, which are a small fraction of the total.

An optimistic estimate of the improvement yielded by pre-selecting target stars results from assuming that all giant stars can be removed from the sample before the search for transiting objects begins. In this case, we estimate the total observing effort needed for false-positive rejection will be about 5% smaller for imaging, and about 10% smaller for low-precision radial velocities, than if no target selection is done. There would be virtually no change in the amount of required time for highly precise radial velocities. Pre-selection of targets is still worthwhile, because the total amounts of telescope time involved are rather large, and because the brighter targets (for which pre-selection is most practical) are the most interesting ones for later follow-up studies, particularly by JWST. But for purposes of scoping the ground-based follow-up effort, early elimination of giants is relatively unimportant.

6. Masses of Super Earths

Perhaps the most important promise of the TESS mission is that the transiting planets it can find will be orbiting the nearest and brightest stars of a given type. These will thus be the best targets for follow-up observations, such as spectroscopy of planetary atmospheres during transits and secondary eclipses with the James Webb Space Telescope (JWST). Furthermore, TESS will have the sensitivity to reach down to Super Earths and even to a few Earth-sized planets orbiting small stars. The critical step for confirming the smallest planets will be Doppler spectroscopy at the highest possible precision in order to determine planetary masses from the spectroscopic orbits of the host stars. If radii and masses can be determined with accuracies at the level of 5 and 10%, theoretical models suggest that it will be possi-

TABLE 2
FOLLOW-UP OBSERVING RESOURCES NEEDED

Observation	Planets	MS EB	Giant EB	LOS Triple	Phys. Triple	# of Targets	Observing Time
Examine TESS Light Curves	1687	2111	40	7237	2080	13155	–
Seeing-Limited Imaging	1687	1689	32	724	1872	6004	3002h 0.5m-1m
Single Spectrum (Classification)	1687	1689	32	72	1872	5352	803h 1m-2m
6 Radial Velocity Spectra (km s^{-1})	1687	1435	10	43	1123	4298	2149h 1m-2m
High-Quality Light Curve	1687	72	2	16	404	2181	10906h 0.5m-1m
4 High-Quality RV Spectra	1687	29	1	6	162	1885	3769h 2m-4m

ble to deduce the structure and composition of Super Earths, namely planets with a family resemblance to Earth, for example to distinguish between desert rocky planets and water worlds. Measuring masses for even the nearest and brightest examples of Super Earths will push the limits of the present state-of-the art spectrometers, such as HARPS on the 3.6-m telescope at the European Southern Observatory and HIRES on Keck 1, which can now reach 1 m s^{-1} on slowly-rotating and inactive solar-type stars. However, many observations are needed to average out astrophysical effects, and mass determinations for transiting Super Earths will be very expensive in telescope time. For example, for an allocation of 75 nights on HARPS and a strategy that focuses on deriving masses for the most interesting small planets, we estimate a yield of perhaps two or three dozen mass determinations. The exciting prospect is that the best of these planets may enable the iconic detection with JWST of biologically interesting molecules in the atmosphere of a habitable planet.

We are grateful to the Vulcan, TrES, and HAT extrasolar planet survey teams for providing us with nearly 1000 candidate transiting planet systems. Their work has led to the discovery of many transiting planets, has provided the training set for development of our follow-up procedures, and is the basis for most of the numerical estimates in §5. DWL thanks the Kepler Mission for partial support of this work through NASA Cooperative

Agreement NCC2-1390.

REFERENCES

- Alonso, R., Deeg, H. J., Brown, T. M., & Belmonte, J. A. 2004, *Stellar Structure and Habitable Planet Finding*, 538, 255
- Alonso, R., et al. 2004, *ApJ*, 613, L153
- Baglin, A., Auvergne, M., Barge, P., Michel, E., Catala, C., Deleuil, M., & Weiss, W. 2007, *Fifty Years of Romanian Astrophysics*, 895, 201
- Bakos, G., Noyes, R. W., Kovács, G., Stanek, K. Z., Sasselov, D. D., & Domsa, I. 2004, *PASP*, 116, 266
- Brown, T. M. 2003, *ApJ*, 593, L125
- Drake, A. J. 2003, *ApJ*, 589, 1020
- Høg, E., et al. 2000, *A&A*, 355, L27
- Ida, S., & Lin, D. N. C. 2005, *ApJ*, 626, 1045
- Koch, D. G., Borucki, W., Webster, L., Dunham, E., Jenkins, J., Marriott, J., & Reitsema, H. J. 1998, *Proc. SPIE*, 3356, 599
- Johnson, J. et al. 2008, submitted, (astro-ph 0829-0029)
- Koch, D. G., et al. 2004, *Proc. SPIE*, 5487, 1491
- Latham, D. W., et al. 2008, *ApJ*, submitted (astro-ph 0812.1161)

Mandushev, G., et al. 2005, ApJ, 621, 1061
Marcy, G., et al. 2005, Progress of Theoretical
Physics Supplement, 158, 24
O'Donovan, F. T., et al. 2006, ApJ, 644, 1237
O'Donovan, F. T., et al. 2007, ApJ, 662, 658
Udry, S., & Santos, N. C. 2007, ARA&A, 45, 397
Walker, G., et al. 2003, PASP, 115, 1023
Winn, J., et al. 2007, AJ, 657, 1098
Skrutskie, M. F., et al. 2006, AJ, 131, 1163